

Autoradiographic Analysis of Diaminopimelic Acid Incorporation in Filamentous Cells of *Escherichia coli*: Repression of Peptidoglycan Synthesis around the Nucleoid

EGBERT MULDER* AND CONRAD L. WOLDRINGH

Department of Molecular Cell Biology, Section of Molecular Cytology, University of Amsterdam,
Plantage Muidergracht 14, 1018TV Amsterdam, The Netherlands

Received 2 January 1991/Accepted 28 May 1991

Peptidoglycan synthesis rate in nonconstricting filaments of *Escherichia coli* *dnaX*(Ts) has been studied by autoradiography of incorporated [³H]diaminopimelic acid. Analysis of autoradiograms of whole cells and sacculi showed that peptidoglycan is synthesized at a reduced rate in the nucleoid-containing parts of these filaments. The lower rate of peptidoglycan synthesis in the cell center coincides with a higher local rate of protein synthesis. DNA-less cell formation in *dnaX*(Ts), *dnaX*(Ts) *sfiA*, and the *minB* minicell-forming mutant is accompanied by a local increase in peptidoglycan synthesis at the constriction site.

Elongation of the *Escherichia coli* cell wall has been shown to involve the diffuse incorporation of peptidoglycan (PG) precursors (11, 17), contrary to previous interpretations (12). Constriction between segregated nucleoids, as occurs in wild-type cells and in recovering cell division mutants, is accompanied by a local increase in PG synthesis rate at the constriction site (15, 17, 19). Coordinately with this local increase, the synthesis rate in the lateral wall decreases (1, 10, 17).

E. coli cells normally constrict in the cell center between segregated daughter nucleoids. It has been suggested that constrictions are activated and positioned relative to the segregated nucleoids (2, 19). Recently, we found that in filaments, constrictions are positioned close to replicating nucleoids but are random in filaments with nucleoids that do not replicate (8). These findings lead us to propose a model for constriction positioning, the "nucleoid occlusion model" (8, 18). In this model, a division signal (e.g., a termination protein [5]) is released upon termination of replication from the site of termination and diffuses out from the nucleoid and initiates a constriction at a site where an inhibitory effect of the nucleoids has decreased sufficiently. Such a nucleoid-free space, and thus constriction initiation, occurs only where nucleoids have segregated or, as in some mutants, between nucleoid and cell pole (7).

The model thus assumes that the presence of nucleoids prevents the cell from constriction. By what mechanism could this occlusion be effectuated? Since constriction is accompanied by an increase in PG synthesis, the nucleoids might inhibit constriction by repression of PG synthesis. We investigated whether nucleoids influence the PG synthesis rate by autoradiographic analysis of diaminopimelic acid (DAP) incorporation in the cell wall of *dnaX*(Ts) filaments growing at 42°C. These cells grow into filaments with a central nucleoid and long nucleoid-free cell ends (8), thus providing a system with a clear difference between nucleoid-containing and nucleoid-free cell parts. Here, we demonstrate an increase in PG synthesis rate in the nucleoid-free parts of these filaments.

Constriction between nucleoids and a cell pole results in

the formation of DNA-less cells. Filaments of the *dnaX*(Ts) mutant, when recovering from a temperature shift, form DNA-less cells by constricting at a site close to the replicating nucleoids; nonreplicating *dnaX*(Ts) *sfiA* filaments growing at the restrictive temperature constrict randomly in the nucleoid-free cell ends (8). Are these constrictions also accompanied by a local increase in PG synthesis at the constriction site? Minicell formation in the *minB* mutant occurs at or close to the cell poles, either in the lateral cell wall or on the polar cap, resulting in minicells of various sizes (3, 9). Are these regular constrictions or are minicells pinched off, not requiring synthesis of new envelope material? In this article, we show that DNA-less cell formation by the recovering *dnaX*(Ts) replication mutant, as well as minicell formation by the *minB* mutant, involves a local increase in PG synthesis rate at the constriction site.

(Preliminary results have been presented at the European Molecular Biology Organization workshop "The Bacterial Cell Cycle: Structural and Molecular Aspects" [October 1990, Collonges-la-Rouge, France] and will appear as a discussion forum in the 5th Forum in Microbiology in Research in Microbiology.)

MATERIALS AND METHODS

Bacterial strains and growth conditions. *E. coli* strains used in this study are listed in Table 1. The cells were cultured under steady-state conditions at 30 or 37°C in minimal medium (13) supplemented with glucose (0.4%) as the sole carbon source, thiamine (4 µg/ml), and required amino acids (50 µg/ml). *dnaX*(Ts) *leu* cells were cultured in the presence of 2.5 µg of leucine per ml; leucine starvation began at an optical density at 450 nm of 0.2. The osmolality of the medium was adjusted to 300 mOsm by the addition of 0.1 M NaCl. Temperature shifts were carried out by diluting the steady-state culture (optical density at 450 nm of 0.2 to 0.3) into prewarmed medium four times for a shift from 30 to 42°C and two times for a shift back from 42 to 30°C.

Pulse-labeling and preparation for autoradiography of cells and sacculi. After 2 h of restrictive growth, *dnaX*(Ts) filaments were pulse-labeled for 4 to 8 min with 20 µCi of *meso*-3,4,5-[³H]diaminopimelic acid (DAP, 25 µCi/mmol; final concentration, 10 µCi/ml; CEA, Gif-sur-Yvette,

* Corresponding author.

TABLE 1. *E. coli* K-12 strains used in this study

Strain	Genotype	Source or reference
LMC500	F ⁻ <i>araD139</i> Δ (<i>argF-lac</i>) <i>U169 deoC1 flbB5301</i> <i>lysA ptsF25 rbsR relA1</i> <i>rpsL150</i>	14
LMC1011	LMC500 <i>minB zcf::Tn5</i>	P1(GC7115) \times LMC500
LMC1012	LMC500 <i>dnaX2016(Ts)</i> <i>zba::Tn10</i>	P1(LMC722) \times LMC500
LMC1013	LMC1012 <i>sfiA::Tn5 pyrD</i>	P1(LMC605) \times LMC1012
LMC249	LMC1012 <i>leu::Tn5</i>	P1(LMC502) \times LMC1012
LMC502	LMC500 <i>leu::Tn5</i>	14
LMC605	LMC500 <i>sfiA::Tn5</i>	8
LMC722	F ⁻ <i>dnaX2016(Ts) gal lac</i> <i>rpsL thi zba::Tn10</i>	8
GC7115	F ⁻ <i>deo minB sfiA85</i> <i>zcf::Tn5</i>	3

France). *dnaX(Ts) leu* cells were labeled at a point near leucine starvation, 105 min after the shift to 42°C, in a 0.25- to 1-min pulse with 80 μ Ci of [³H]leucine (137 μ Ci/mmol; final concentration, 80 μ Ci/ml; CEA) and in a 10- to 15-min pulse with [³H]DAP. Cells labeled with [³H]DAP were fixed with 0.1% OsO₄, and [³H]leucine-labeled cells were fixed with 10% trichloroacetic acid and 2.5% glutaraldehyde. Fixed cells were prepared by agar filtration (12) for autoradiography. For the preparation of sacculi, 2 ml of the labeled cells was mixed with 667 μ l of 10% sodium dodecyl sulfate at 80°C and subsequently boiled for 1 h. The cells were left to lyse at 80°C for 36 h and were agar filtrated and prepared for autoradiography as described by Woldringh et al. (17).

Autoradiography. Autoradiography of cells and sacculi that had incorporated [³H]DAP or [³H]leucine, photography, and analysis of silver grain distributions were carried out as described previously (17).

Genetic techniques. P1 *vir*-mediated transduction was carried out as described by Miller (6). Temperature sensitivity of the strains was tested on Luria broth plates without NaCl at 42°C and on Luria broth plates with 0.5% NaCl at 30°C.

Microscopy. Fluorescence microscopy and analysis of nucleoid positions of *dnaX(Ts)* filaments were performed as described by Mulder and Woldringh (8) and Mulder et al. (7). However, the preparation of cells for fluorescence microscopy was improved. Instead of drying cells on a polylysine-coated glass slide, a smooth agar surface was prepared by pipetting 50 μ l of 2% agarose at 45°C under a coverslip. After gelation of the agarose, the coverslip was removed and 1 μ l of concentrated cell suspension was applied to the agarose surface, spread out under a second coverslip, and sealed off with nail polish.

RESULTS

PG synthesis rate along the length of nonconstricting *dnaX(Ts)* filaments. To answer the question of whether the presence of nucleoids influences PG synthesis, we analyzed DAP incorporation in *dnaX(Ts)* cells growing at 42°C. As DNA replication halted and cell growth continued at the restrictive temperature, these cells grew into filaments with centrally located nucleoids. An increasing percentage of the nucleoids contracted during the 42°C shift (for a more detailed description of cell division and nucleoid morphology of this mutant, see reference 8). After two mass doublings at 42°C, *dnaX(Ts)* filaments were pulse-labeled for 4 to 8 min with [³H]DAP. Figure 1 shows an autoradiogram of *dnaX(Ts)* filaments. The analysis of grain positions over these filaments resulted in the grain distribution in Fig. 2B: it shows a central dip, which was reproduced in three independent experiments. In these experiments, [³H]DAP incorporation, and thus PG synthesis rate, was reduced 20 to 30% in the central, nucleoid-containing parts of the filaments compared with that in the nucleoid-free cell ends. In the experiment whose results are shown in Fig. 2B, the coefficient of variation of the number of grains per section of normalized cell length ranged from 10 to 19%, averaging 14%. For three positions, this variation has been indicated in the figure by two-sided error bars. The extent of the increase in rate of PG synthesis in the nucleoid-free parts of the filaments becomes clearer when comparing this grain distribution with that of

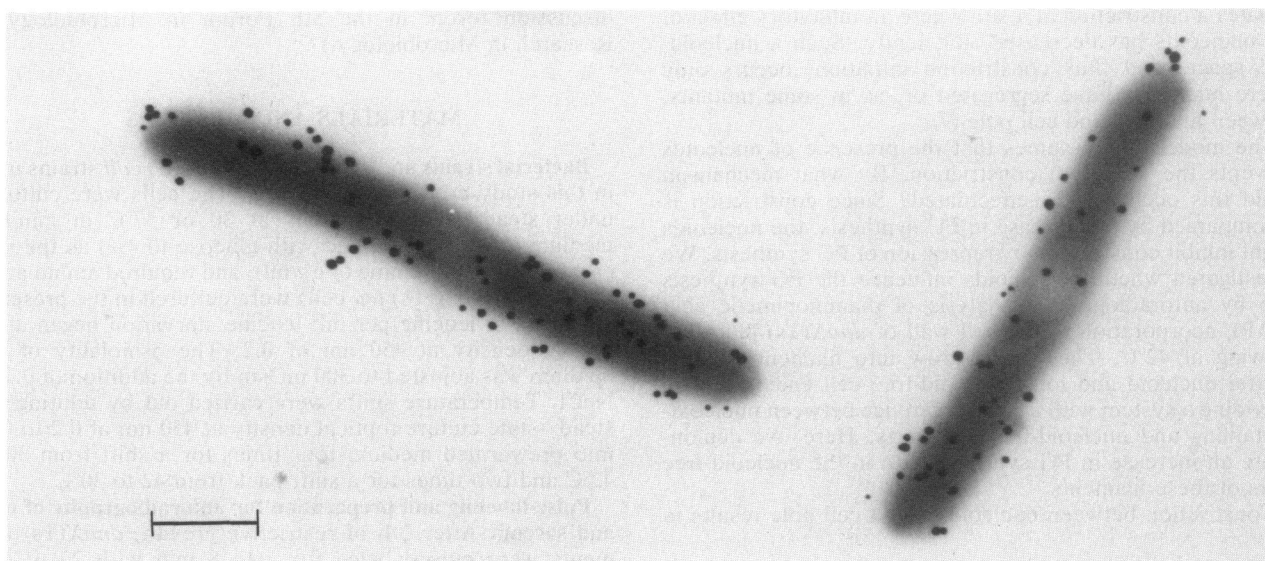


FIG. 1. Autoradiogram of [³H]DAP incorporated after pulse-labeling in *dnaX(Ts)* filaments grown for two mass doublings at 42°C. Bar, 1 μ m.

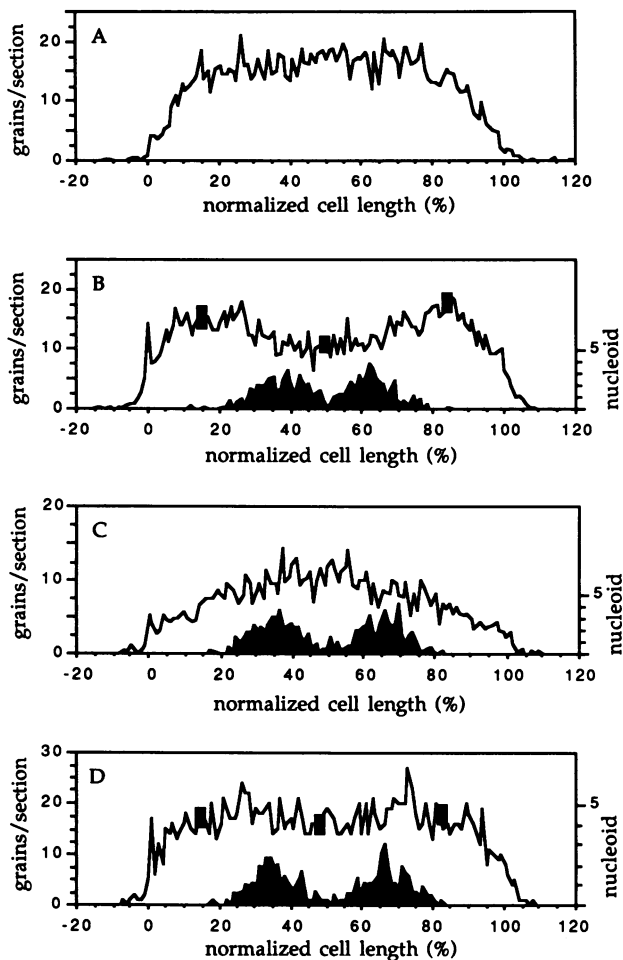


FIG. 2. Autoradiography of [^3H]DAP incorporated in *ftsZ*(Ts) and *dnaX*(Ts) filaments and of [^3H]leucine in *dnaX*(Ts) *leu* filaments. In the grain distributions, the total number of grains per section of normalized cell length, added up for all cells, is plotted against a normalized cell length of 1 μm , with sections of 0.01 μm . The grain distributions in DAP autoradiograms of (A) *ftsZ*(Ts) filaments grown for two mass doublings at 42°C ($n = 125$) [from reference 16] remeasured with new equipment) and of (B) *dnaX*(Ts) filaments grown for two mass doublings at 42°C ($n = 150$) are shown. The variation of the number of grains per section of normalized cell length, for three points, is shown by two-sided error bars, which indicate the standard deviation of the distribution of grains in these sections. Grain distribution in leucine autoradiograms of *dnaX*(Ts) *leu* filaments grown for 105 min at 42°C ($n = 275$) (C) and that in DAP autoradiograms of the same *dnaX*(Ts) *leu* cells ($n = 400$) (D) are shown. Distributions of extremities of nucleoids, measured from OsO_4 -fixed cells, are indicated by the shaded area.

nonconstricting, *ftsZ*(Ts) filaments with well-separated nucleoids (Fig. 2A), which is uniform.

Superimposed on the grain distribution in Fig. 2B is the distribution of nucleoid extremities, measured from fluorescence micrographs of OsO_4 -fixed, 4,6-diamido-2-phenylindole-stained cells from the same culture. Comparison of both distributions indicates that the central dip in the PG synthesis rate coincides with the nuclear region of the filaments. Preliminary observations of nucleoids stained with 4,6-diamido-2-phenylindole in living cells indicated that the nucleoids are somewhat larger in unfixed cells. The present boundaries, however, still represent the bulk of the DNA.

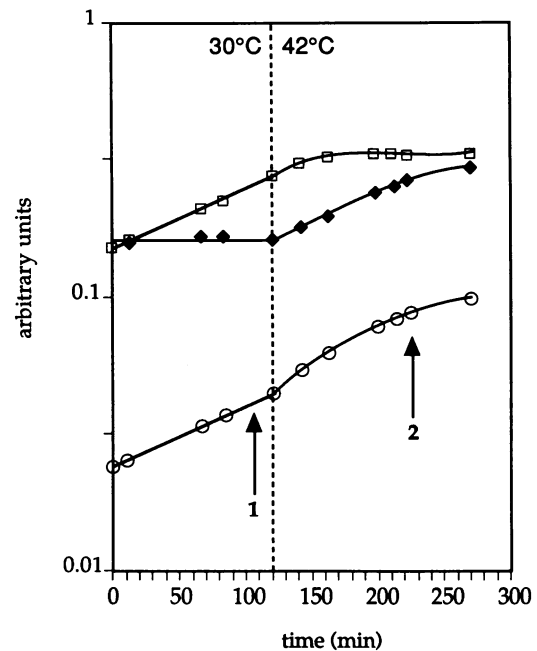


FIG. 3. (A) Growth and cell division of the *dnaX*(Ts) *leu* mutant in minimal GB1 medium with 2.5 μg of leucine per ml; optical density at 450 nm (\circ), cell number (\square), and average cell mass (\blacklozenge) are depicted. The *dnaX*(Ts) *leu* cells growing at steady state at 30°C were pulse-labeled with [^3H]DAP for autoradiography (arrow 1). These cells were then shifted from 30 to 42°C (dotted line) and pulse-labeled for autoradiography with [^3H]leucine or [^3H]DAP at a point near leucine starvation (arrow 2).

To exclude the possibility that the shape of the cell on the supporting surface was affecting the silver grain distribution (the cell ends are bulbous and have a depression at the site of the nucleoid), an independent experiment was performed in which the [^3H]DAP incorporation in whole *dnaX*(Ts) cells was compared with that in isolated sacculi, which are completely flat; again, a central dip was obtained (result not shown).

Protein synthesis rate along *dnaX*(Ts) *leu* filaments. To investigate whether the increase in PG synthesis rate correlated with an increase in protein synthesis rate in the nucleoid-free regions, the rate of [^3H]leucine incorporation along *dnaX*(Ts) *leu* filaments was analyzed by autoradiography. To be able to apply very short pulses of [^3H]leucine and to attain a high specific activity, the pulse-labeling experiment was performed with a *dnaX*(Ts) *leu* mutant at a point near leucine depletion of the medium, at 42°C. In Fig. 3, growth and cell division characteristics of this mutant during a shift experiment (30 to 42°C) are shown. The grain distribution in autoradiograms of *dnaX*(Ts) *leu* filaments pulse-labeled for 15 s with [^3H]leucine shows (Fig. 2C) that protein synthesis was highest in the cell center and decreased toward the poles. Figure 2D shows that the same *dnaX*(Ts) *leu* cells pulse-labeled for 10 to 15 min with [^3H]DAP again showed a centrally decreased PG synthesis rate. The central dip, estimated at 15 to 20%, was smaller than that in Fig. 2B, which may be due to the longer pulse-labeling time. The number of grains per section of normalized cell length had a variation similar to that in Fig. 2B.

The higher PG synthesis rate in nucleoid-free cell ends of *dnaX*(Ts) *leu* cells does not correlate with an increased rate

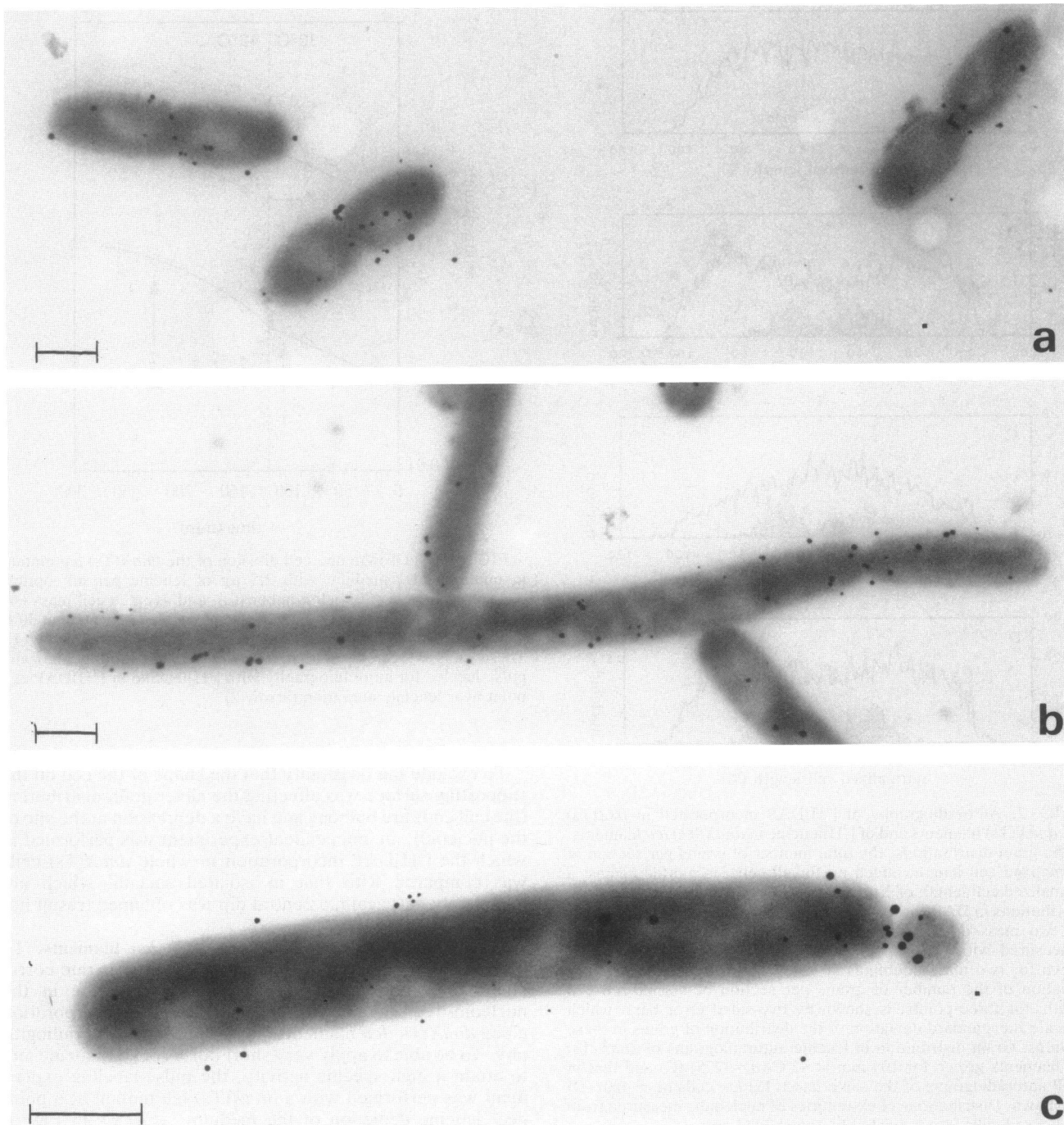


FIG. 4. Autoradiograms of *dnaX(Ts)* cells growing in steady state at 30°C (a), *dnaX(Ts)* filaments recovering from a temperature shift (b), and *minB* filaments growing at steady state at 37°C (c). Bar, 1 μ m.

of protein synthesis in these nucleoid-free cell parts. On the contrary, the centrally decreased PG synthesis rate coincides with the highest rate of protein synthesis.

PG synthesis rate in the lateral cell wall of constricting filaments. As in wild-type cells, constriction in *dnaX(Ts)* *leu* cells growing at 30°C is accompanied by a local increase in PG synthesis at the constriction site (Fig. 4a and 5A and B). Does this also hold for constrictions that produce DNA-less cells, as for instance in recovering *dnaX(Ts)* filaments and in

dnaX(Ts) *sfiA* filaments at 42°C in the absence of SOS division inhibition? Filaments of the *dnaX(Ts)* mutant, which had been growing for two mass doublings at 42°C, were shifted back to 30°C (for a detailed description, see reference 8) and after 2.5 h were pulse-labeled for 4 to 8 min with [³H]DAP. An autoradiogram of [³H]DAP incorporated into these DNA-less cell-forming *dnaX(Ts)* filaments, shown in Fig. 4b, shows that the PG synthesis rate is locally increased at the constriction site, just as in wild-type cells

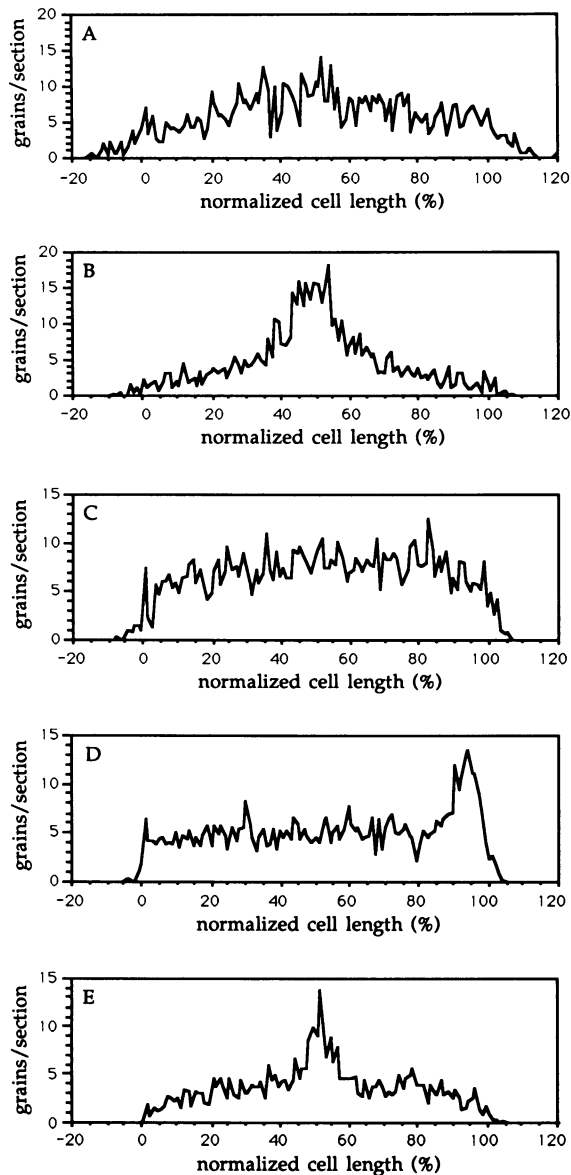


FIG. 5. Autoradiography of [^3H]DAP incorporated in *dnaX(Ts)* cells growing in steady state at 30°C. The grain distribution was determined in autoradiograms with (A) nonconstricting cells and (B) centrally constricting cells (total of 350 cells). (C through E) Autoradiography of [^3H]DAP incorporated in *minB* cells growing at steady state at 37°C. The grain distribution was determined in autoradiograms of (C) nonconstricting cells, (D) polarly constricting cells, and (E) centrally constricting cells (total of 400 cells).

(Fig. 4a). The same holds true for DNA-less-cell-forming *dnaX(Ts) sfiA* cells growing at 42°C (result not shown). Minicell formation often gives the impression that a simple pinching-off mechanism takes place. However, minicell formation in *minB* cells (Fig. 4C), like normal constrictions, also involves a local increase in PG synthesis at the constriction site. The analysis of the average grain distribution in *minB* filaments, in Fig. 5D, shows the increased synthesis rate at minicell constriction sites as polar peaks.

In conclusion, both DNA-less cell and minicell formations are accompanied by a local increase in rate of PG synthesis

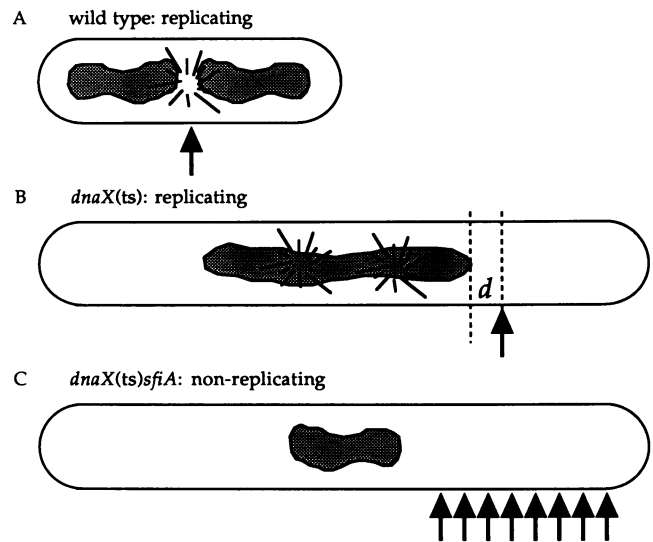


FIG. 6. Constriction positioning in replicating and nonreplicating *E. coli* cells. In replicating cells (A and B), constriction occurs at the nearest site where the negative nucleoid effect has decreased sufficiently, just outside the nucleoid region (arrows); in nonreplicating filaments (C), constrictions are positioned randomly.

at the constriction site, similar to normal division in wild-type cells.

DISCUSSION

Increased PG synthesis rate in the nucleoid-free parts of *dnaX(Ts)* filaments: the "negative nucleoid effect." We have shown that *dnaX(Ts)* filaments with centrally located nucleoids, growing at 42°C, incorporate DAP at a reduced rate in the nucleoid-containing parts of the cell. We have shown that the silver grain distribution of these filaments was not affected by the cell shape (bulbous ends and a depression in the cell center) on the supporting surface and that the lower rate of PG synthesis in the cell center correlated with a higher rate of protein synthesis. We suggest that the inhibitory effect of nucleoid presence (the so-called "negative nucleoid effect") may be due to the transcriptional and translational activities for the production of a labile repressor protein (see below). Apart from such a direct effect of the nucleoid, it could be envisaged that a lower availability of substrates in the nucleoid-containing parts of the filaments may contribute to the reduced rate of PG synthesis in these cell parts.

The nucleoid occlusion model. Initiation of constriction is accompanied by an increase in PG synthesis at the constriction site (11, 15). We propose that the repression of PG synthesis by the nucleoid prevents the cell from constricting in the nuclear region by prohibiting the increase in PG synthesis that is needed for constriction initiation. Repression of PG synthesis around the nucleoid should be a short-range effect, which may be achieved through transcription and/or translation activities of the nucleoid or through the synthesis of a labile repressor protein. We speculate that when replication terminates, a positive division signal is released and diffuses out from the nucleoid into the cell (8). The negative nucleoid effect on PG synthesis, however, prevents this signal from initiating constriction until the nucleoids are properly segregated (Fig. 6A). Only then is this

signal able to overrule the negative nucleoid effect and initiate a constriction between the segregated nucleoids. In this way, it is the local tipping of the balance between the positive and negative effectors of PG synthesis that determines timing and positioning of constriction initiation.

Anucleate cell formation in the nucleoid occlusion model. Filaments of *dnaX(Ts)* recovering from a temperature shift form DNA-less cells by constricting, preferentially at a site close to the nucleoid (8). In the nucleoid occlusion model, this positioning effect is explained by assuming that the hypothetical division signal, which is produced by the replicating nucleoids at termination, diffuses out into the cell and initiates a constriction at the nearest site where the negative nucleoid effect is reduced sufficiently. This is just outside the nucleoid region (Fig. 6B). Constriction positioning with anucleate cell formation in nonreplicating filaments, e.g., in *dnaX(Ts) sfiA* at 42°C, is random within the nucleoid-free cell ends (8) (Fig. 6C). Unlike DNA-less cell formation in *dnaX(Ts)* filaments, this type of division is replication independent, it is inefficient (8), and it requires the cyclic AMP-cyclic AMP receptor protein complex (4). However, both types of division involve a local increase in PG synthesis at the constriction site. Filamentation of *dnaX(Ts) sfiA* cells results in the formation of nucleoid-free space in which PG synthesis would be increased. Could this increase cause the initiation of constriction? We speculate that in *dnaX(Ts) sfiA* filaments at 42°C, constrictions may occur spontaneously, through facilitation by the increased PG synthesis rate in the nucleoid-free region.

From this study, it appears that local regulation of PG synthesis rate may play an important role in initiation and positioning of constrictions in *E. coli*.

ACKNOWLEDGMENTS

We thank Nanne Nanninga for critically reading the manuscript, Norbert Vischer for writing the software for the analysis of autoradiograms, and Mohamed El'Bouhali for the autoradiographic analysis of the *minB* mutant. We also thank Frans Wientjes and Peter Huls for discussion and assistance.

REFERENCES

1. Cooper, S. 1988. Where and when is the cell wall peptidoglycan of gram-negative bacteria synthesized?, p. 79–90. In P. Actor, L. Daneo-Moore, M. L. Higgins, M. R. J. Salton, and G. D. Shockman (ed.), Antibiotic inhibition of bacterial cell surface assembly and function. American Society for Microbiology, Washington, D.C.
2. Hussain, K., K. J. Begg, G. P. C. Salmond, and W. D. Donachie. 1987. Par D: a new gene coding for a protein required for chromosome partitioning and septum localization in *Escherichia coli*. *Mol. Microbiol.* **1**:73–81.
3. Jaffé, A., R. D'Ari, and S. Hiraga. 1988. Minicell-forming mutants of *Escherichia coli*: production of minicells and anucleate rods. *J. Bacteriol.* **170**:3094–3101.
4. Jaffé, A., R. D'Ari, and V. Norris. 1986. SOS-independent coupling between DNA replication and cell division in *Escherichia coli*. *J. Bacteriol.* **165**:66–71.
5. Jones, N. C., and W. D. Donachie. 1973. Chromosome replication, transcription and cell division in *Escherichia coli*. *Nature (London)* **243**:100–103.
6. Miller, J. H. 1972. Experiments in molecular genetics. Cold Spring Harbor Laboratory, Cold Spring Harbor, N.Y.
7. Mulder, E., M. El'Bouhali, E. Pas, and C. L. Woldringh. 1990. The *Escherichia coli minB* mutation resembles *gyrB* in retarded nucleoid segregation and decreased negative supercoiling of plasmids. *Mol. Gen. Genet.* **221**:87–93.
8. Mulder, E., and C. L. Woldringh. 1989. Actively replicating nucleoids influence positioning of division sites in *Escherichia coli* filaments forming cells lacking DNA. *J. Bacteriol.* **171**:4303–4314.
9. Mulder, E., and C. L. Woldringh. Unpublished data.
10. Nanninga, N., F. B. Wientjes, B. L. B. DeJonge, and C. L. Woldringh. 1990. Polar cap formation during cell division in *Escherichia coli*. *Res. Microbiol.* **141**(1):103–118.
11. Nanninga, N., and C. L. Woldringh. 1985. Cell growth, genome duplication and cell division, p. 259–318. In N. Nanninga (ed.), *Molecular cytology of Escherichia coli*. Academic Press, Inc., New York.
12. Ryter, A., Y. Hirota, and U. Schwarz. 1973. Process of cellular division in *Escherichia coli*: growth pattern of *E. coli* murein. *J. Mol. Biol.* **78**:185–195.
13. Taschner, P. E. M., P. G. Huls, E. Pas, and C. L. Woldringh. 1988. Division behavior and shape changes in isogenic *fstZ*, *ftsQ*, *ftsA*, *pbpB*, and *ftsE* cell division mutants of *Escherichia coli* during temperature shift experiments. *J. Bacteriol.* **170**:1533–1540.
14. Taschner, P. E. M., J. G. J. Verest, and C. L. Woldringh. 1987. Genetic and morphological characterization of *ftsB* and *nrdB* mutants of *Escherichia coli*. *J. Bacteriol.* **169**:19–25.
15. Wientjes, F. B., and N. Nanninga. 1989. Rate and topography of peptidoglycan synthesis during cell division in *Escherichia coli*: concept of a leading edge. *J. Bacteriol.* **171**:3412–3419.
16. Woldringh, C. L., M. A. de Jong, W. van den Berg, and L. Koppes. 1977. Morphological analysis of the division cycle of two *Escherichia coli* substrains during slow growth. *J. Bacteriol.* **131**:270–279.
17. Woldringh, C. L., P. Huls, E. Pas, G. J. Brakenhoff, and N. Nanninga. 1987. Topography of peptidoglycan synthesis during elongation and polar cap formation in a cell division mutant of *Escherichia coli* MC 4100. *J. Gen. Microbiol.* **133**:575–586.
18. Woldringh, C. L., E. Mulder, J. A. C. Valkenburg, F. B. Wientjes, A. Zaritsky, and N. Nanninga. 1990. Role of the nucleoid in the toporegulation of *Escherichia coli*. *Res. Microbiol.* **141**:39–49.
19. Woldringh, C. L., J. A. C. Valkenburg, E. Pas, P. E. M. Taschner, P. Huls, and F. B. Wientjes. 1985. Physiological and geometrical conditions for cell division in *Escherichia coli*. *Ann. Inst. Pasteur/Microbiol.* **136A**:131–138.